Effects of Non-Essential Protein On D-Glucose to Control Diabetes: DFT Approach

Shreya Tiwary
Govt. D.B.Girls' P.G. Autonomous College Library: Government Dudhdhari Bajrang Girls' Post-Graduate Autonomous College Library

Hemant Kumar
Pandit Ravishankar Shukla University

Mohan L Verma (cmprlssi@yahoo.com)
Shri Shankaracharya College of Engineering and Technology: SSGI Faculty of Engineering and Technology https://orcid.org/0000-0001-6628-9888

Deepti Pateria
Pandit Ravishankar Shukla University

Research Article

Keywords: Glc-arg, Glc-cys, density functional theory, SIESTA, diabetes, amino acids

Posted Date: November 17th, 2021

DOI: https://doi.org/10.21203/rs.3.rs-1038099/v1

Version of Record: A version of this preprint was published at Journal of Molecular Modeling on January 25th, 2022. See the published version at https://doi.org/10.1007/s00894-021-05013-7.

Effects of Non-essential Protein on D-glucose to control Diabetes : DFT Approach

Shreya Tiwary[1], Hemant Kumar[2], Mohan L. Verma[3], Deepti Pateria[4]
[1]Govt. Dudhdhari Bajrang Girls' Post-Graduate Autonomous College, Raipur, Chhattisgarh, India, 492010
[2]Center for Basic Sciences, Pt. Ravishankar Shukla University, Amanaka, Raipur, Chhattisgarh, India, 492010
[3]Department of Applied Physics, FET-SSGI, Shri Shankaracharya Technical Campus, Junwani, Bhilai, Chhattisgarh, India 490020
[4]School of Studies in Physics and Astrophysics, Pt. RaviShankar Shukla University, Raipur

Abstract

Diabetes is a disease found in every 1 out of 4 people in the world. The glucose molecule is one of the sources of energy in the body and the lack of the digestion of glucose causes diabetes type 1 and type 2. Arginine and Cysteine is a nonessential amino acid that contains sulfur and help to maintain the metabolisms of humans. We explored the Glucose-Arginine (Glc-arg) and Glucose-Cysteine (Glc-cys) molecules by finding their structural properties, electronic properties, chemical reactivity, mechanical strength and transport properties because these non-essential amino acids molecules inhibit glucose-stimulated insulin secretion. Density functional theory (DFT) have been implemented to study all the properties of Glc-arg and Glc-cys using SIESTA software. Glucose-Arginine (Glc-arg) inhibits a large percentage of glucose secretion and shows high chemical reactivity.

Keywords

Glc-arg, Glc-cys, density functional theory, SIESTA, diabetes, amino acids

1. Introduction

Carbohydrates are widely found in nature, from unicellular organisms like bacteria to multicellulars like plants, animals, and even fungi. Out of the different kinds of carbohydrates present, glucose is the primary form of carbohydrate found in the living organism, produced by photosynthetic plants [1]. Glucose constitutes six carbon atoms, twelve hydrogen atoms, and six oxygen atoms linked together through covalent bonds with the chemical formula C6H12O6. Being the ultimate source of energy on this planet, it is available for every organism, plant, and animal both [2]. During the process of glycolysis, glucose is breakdown into the pyruvate end product, which ultimately undergoes either the Krebs cycle or the Cori cycle, and ATP, the currency of energy, is formed. Glucose has two enantiomers including, D-glucose and L-glucose, but the former one is dominant in the universe whose presence can be determined by standard methods [3].

Amino acids are made up of organic compounds containing amine groups and carboxylic acids that form the basic unit structure of proteins. Due to the peptide bond formation, amino acids are linked together to form the protein [4]. These proteins are found in the cell membrane, hormones, cell organelles, enzymes, organs, skin, bones, brain, liver, and many more [5]. There are 20 amino acids found to prepare proteins, and these amino acids are classified into two types of amino acids: essential amino acids and non-essential amino acids. Essential amino acids are those which are not synthesized in our body specifically, histidine, isoleucine, leucine, lysine, methionine, phenylalanine, threonine, tryptophan, and valine, and they are obtained through the food we eat[6]. On the other hand, non-essential amino acids are those, which are synthesized by our body, mainly through glucose, and include alanine, asparagine, aspartate, cysteine, glutamate, glutamine, glycine, proline, serine, tyrosine, and arginine [7].

In this paper, we are going to consider the non-essential amino acids that include Arginine (Arg) and Cysteine (Cys) and study their interaction with the carbohydrate i.e, glucose (Glc) through the Maillard reaction. Arginine and cysteine are the amino acids formed in our body and play a vital role in the regulation of glucose, and hence affecting the sugar level concerning diabetes. Diabetes is a metabolic disorder that is caused due to inefficiency in insulin secretion or inadequate insulin action, or both, that results in hyperglycemia. Insulin is a hormone (secreted by the pancreas) that plays a very important to regulate the glucose level in our body, but the hyperglycemia condition affects the liver, kidneys, eyes, nerves, and even the heart [8]. There are three types of diabetes i. e, Type 1 diabetes, Type 2 diabetes, and Gestational diabetes. Type 1 diabetes, also called Insulin-Dependent Diabetes Mellitus (IDDM), is caused due to autoimmune destruction where the beta cell of the

* Corresponding author. Tel.: +91-9303452648
E-mail address: cmprlssi@yahoo.com (Mohan L. Verma).

pancreas is attacked by the T cell-mediated response, which ultimately leads to disturbance in insulin level [9]. Type 2 diabetes, also referred to as the Non-Insulin-Dependent Diabetes Mellitus (NIDDM) that is initiated with insulin resistance, cells under this condition do not respond to the insulin made by pancreatic beta cells effectively [10]. This resistance increases with an increase in the demand for insulin in target cells like adipose tissue, skeletal muscles, and liver cells. Gestational diabetes can be seen in pregnant women with high glucose levels, but it is treatable in some cases [11].

Maillard reaction is a complex process, where there is a condensation reaction in the presence of heat between amino acids and reducing sugar with no enzymes involved. During the reaction, a Schiff's base is formed that is very unstable and later is rearranged as an Amadori product, the first product of the Maillard reaction, which then proceeds to enolization [12]. Depending on pH, temperature, and substrate various products from Maillard reactions can be obtained [13]. Considering the substrates here, Arg and Cys were allowed to interact with the glucose (reducing sugar), and as a result of this condensation reaction, water molecules are released during the reaction, and Glc-Arg and Glc-Cys molecules are formed, respectively. The synthesis process of Glucose-arginie and Glucose-cysteine molecules is shown in Figure 1, in which D-glucose react with non-essential amino acids and formation of water molecules and Glc-arg and Glc-cys products are formed.

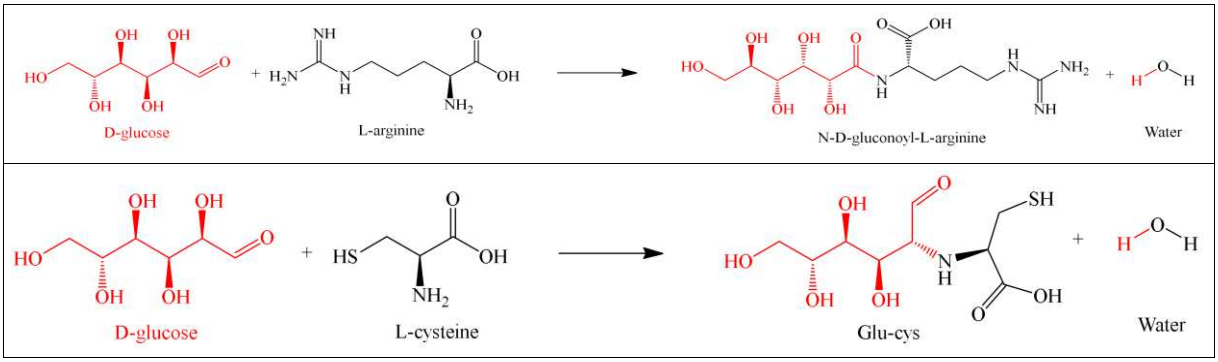

Figure 1: Chemical reaction of synthesis process of (a) Glucose-argine and (b) Glucose-cysteine through Maillard reaction.

The reason behind examining the molecules of Glc-Cys and Glc-Agr is that in the case of arginine, as per the data gathered, it improves the sensitivity of insulin for Type-2 diabetic patients by causing the oxidation of fatty acids and glucose in the adipose tissues. It helps to regulate the glucose level in the body by stimulating the production of glucose-6-phosphate and hence starts insulin secretion [14]. Now consider the case of cysteine and H2S donor NaHS, in which the presence of high K+ inhibits the glucose-induced insulin release from pancreatic cells and MIN6 cells. Cysteine decreases ATP production by glucose [15]. Cysteine also increases the H2S amount in **mouse insulinoma (MIN6 cells)** that reduces insulin production [16]. The conditions where beta cells suffer to produce insulin can be seen in the case of Type 2 diabetes. Therefore the interaction of these two amino acids with the glucose, by Maillard reactions gave us certain results that could be very helpful to understand the stability, configuration, and applications of the molecules formed [17].

2. Methodology

The wave function of each atom in Glc-arg and Glc-cys, as well as their Schrodinger equation equations, are quantified using density functional theory. Consider it a successful single-molecules technique since it gives a functionalization of equilibrium particles based on many-body interactions between particles [18]. This DFT theory is implemented by the SIESTA programme (Spanish Initiative for Electronic Simulations with Thousands of Atoms). The SIESTA uses a basis set of strictly-localized atomic orbitals and employs norm-conserving pseudopotentials [19].

In Jacob's Ladder, general gradient approximation (GGA) is more accurate than the local density approximation (LDA), but due to having a lack of computational efficiency, to reduce complexity, we use open source software SIESTA which works in LDA and GGA functionals [20]. We have implemented Perdew, Burke, and Emzerh's general gradient approximation (GGA) functionals in our proposed work (PBE). The self-consistent field (SCF) energy solutions for the many-body system is not exact, to get precise results of molecules these three parameters firstly optimize mesh-cutoff, k-point and lattice constant. We get the Meshcuttoff of 400 Ry for both Glc-arg and

Glc-cys, which tells the number of plane wave functions being utilized as basis functions to represent the wave function of atoms in molecules. The k-point used for final optimization and all properties calculation is 3*3*3 in both cases, it provides sampling points in the first Brillouin zone of the material. We examine the lattice constant based on total energy because it affects the interatomic distances of Glc-arg and Glc-cys evolved from binding forces and introduced Stress-Strains calculations, the results are 1.2 Å. The aforesaid parameter is used in the final optimization of Glc-arg and Glc-cys, and a typical conjugate-gradient (CG) approach is used, with an interatomic force tolerance between atoms of less than 0.001 eV/Å and a basis set of Double zeta plus polarisation orbitals.

After the final optimization was performed, the optimised geometry was used for further calculation of Ground state energy, Hirshfeld and Vorononi population analysis, bond length, the density of states (DOS) and projected density of states (PDOS). Surface reckoning(ESP and HOMO-LUMO) and population analysis (Mulliken and ZDO) are obtained from the freely licensed software ArgusLab[21]. Stress vs Strain plot has generated from the increasing (elongation) and decreasing (compression) in the length of lattice vectors, the change in length carried out in the interval of 1 per cent of the actual length of lattice vectors.

Electron transport studies of Glc-arg and Glc-cys have been performed using the Transiesta package, which uses the additional Non-Equilibrium Green Function (NEGF) in the density functional theory calculation[22]. The molecules attached with the electrode (conducting bridge for non-metals) in the saturated sandwiched between the left and right electrode. The NEGF approach works under ballistic conduction and solves the non-equilibrium electron distribution of the central region which is Glc-arg and Glc-cys molecules result in their inelastic scattering region.

3. Results and Discussions

3.1 Structural properties analysis

In any system, the calculation for stability is the primary method that tells if the system is worthless or indispensable. To allow the interaction of molecules and observe their applications, the mechanical and thermodynamic stabilities of a system play a significant role. Cohesive energy gives information about the amount of energy required to separate atoms from the molecules or system through which the atoms become neutrally stable or are arranged in a neutral state. When atoms are bonded strongly in a molecule, it represents that their cohesive energy value is large so is their high mechanical strength[23]. The thermodynamical stability of a system depends upon the enthalpy of formation that indicates the change in enthalpy during the reaction which results in the formation of one mole of the product and based on the heat exchange phenomena, the reaction can either be endothermic(absorbed) or exothermic(released)[24]. In table 1. the calculation for stability has been performed for glucose-arginine(Glc-Arg) and glucose-cysteine(Glc-Cys) molecules in which the cohesive energy and enthalpy of formation are calculated in eV/atom. The high negative value of enthalpy of formation shows the strong product formation capability of the compound's elements and the molecules formed are more stable.

Table 1: Stability Calculations

Molecules	Total Energy E_{total} (eV)	Cohesive Energy E_C (eV)	Enthalpy of formation ΔH (eV)
Glucose-Arginine (Glc-arg)	-6940.92	-7.01	-5.47
Glucose-Cystene (Glc-cys)	-5392.79	-6.91	-4.95

$$E_c = \frac{E_{total} - \sum_1 n_i \times E_{atom}^i}{\sum_1 n_i} \quad (1)$$

$$\Delta H = \frac{E_{total} - \sum_1 n_i \times E_{cubic}^i}{\sum_1 n_i} \quad (2)$$

In the case of the Glc-Arg compound, there is a total number of 48 atoms out of which 24 hydrogen atoms, 12 carbon atoms, 4 nitrogen atoms, and 8 oxygen atoms are present whereas, in the Glc-Cys compound there is a

total number of 35 atoms out of which 17 hydrogens atoms, 9 carbon atoms,1 nitrogen atom, 7 oxygen atoms, and 1 sulfur atom which shows their contribution for the calculation of stability. Cohesive energy was calculated by equation 1. and equation 2. can be used to calculate the enthalpy of formation, in which Σni represents the sum of all the atoms present in the molecules and Etotal represents the energy at the ground state of the molecules. In equation 1, Σni × Eiatom represents the product of the summation of atoms of the specific element and the energy of that element in a neutral free state or an isolated state. However, in equation 2. Σni × Eicubic, the Eicubic is the energy of a cubic or solid system of individual elements that are multiplied by a total number of specific atoms present in the molecules.

In Figure 2(a,d). the well-labeled ball and stick diagrams represent Glc-arg and Glc-Cys compounds, respectively. Considering the position of atoms in a molecule, the atomic charge (QC) graphs are plotted for respective atoms that are visible in Figure 3. and Figure 4. for Glc-arg and Glc-Cys, sequentially. In Figure 2(c), the color-coded balls are used for individual elements and this idea of identification is used again during the Electropotential surface map(ESP), HOMO-LUMO surface, and charge density analysis. The alignment of both the molecules in the XZ-plane is perpendicular to the Y-axis that can be explained with the help of Figure 2(b) as it helps to visualize the analysis of charge density and stress-strain calculation in this work.

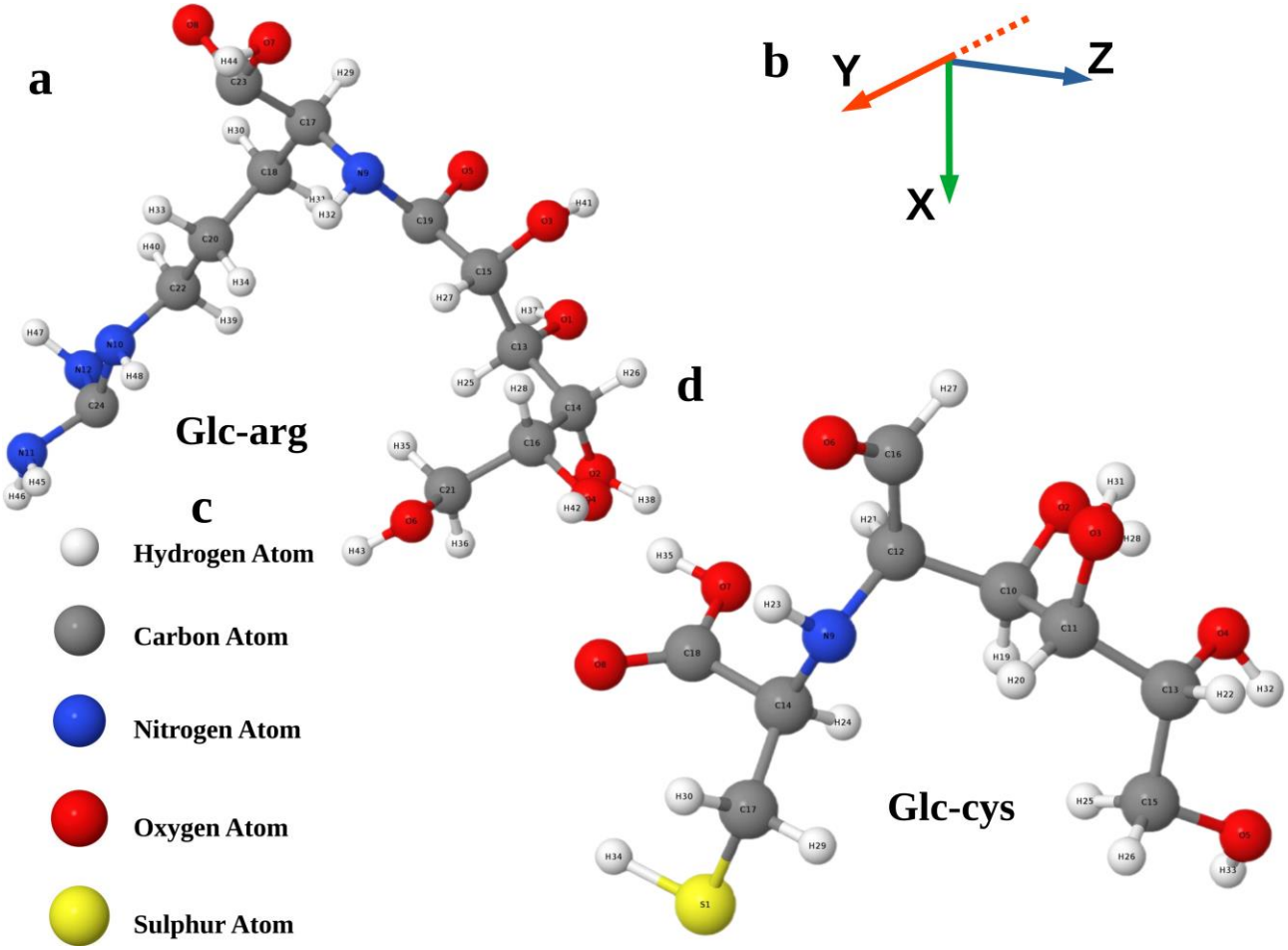

Figure 2: **a** and **d** represents Ball and stick model of Glc-arg and Glc-cys compounds, respectively. **b** represents the cartesian coordinate system and **c** represents the types of atoms present in the compounds.

3.2 Population analysis

In molecules, the population analysis provides quantitative information about the atomic charge contained by the individual atom in molecules. The value of this atomic charge is applied to determine the electron-donating atom, electron-accepting atom, charge distribution, polarity between bonded atoms, charge transfer from interacting molecules, and electronegativity in the molecules. The electron-accepting atom act as a frictional atom in the calculation of transport properties as a hindrance is created in the path whenever there is a flow of negative charges between the left electrode and right electrode and this gives rise to the current. The partial

atomic charge provides important information about molecules [25]. To obtain accurate and trustable charge distribution data in Glc-arg and Glc-Cys compounds, we have applied four different population analysis methods: Mulliken charge, zero differential overlaps (ZDO) charges, Hirsfeld charges, and Vornoi charges.

During the bond formation of molecules, the atomic orbitals of two atoms overlap and form either bonding molecular orbital or antibonding molecular orbital.

The formation of these molecular orbital creates a molecular wave function using nonorthogonal basis sets of functions and presents the Mulliken population analysis. A net population matrix is created by the sum of all occupied molecular orbitals that give information about atomic-orbital populations and overlap populations [26]. The summation of half overlap populations with the atomic orbital populations for each molecular orbital gives a gross population matrix, which gives a Mulliken charge distribution in the atomic orbital.

$$Q_A^{Mulliken} = Z_A - \sum_{\mu \in A} Q_\mu$$

(3)

Z_A = nuclear charge

In Hirshfeld and Voronoi population analysis, electron density plays a vital role that is the function of space and atomic domain, respectively. In the case of Hirshfeld charge, the calculation for an atom works as a function of space estimation and for that, it includes complete molecular electronic density, the atomic density of that specific atom, and fictitious promolecule density [27]. Whereas in the case of Voronoi charge, the calculation is carried out from deformation density that is equal to the difference between the atomic density of that specific atom and fictitious promolecule density.

$$Q_A^{Hirshfeld} = Z_A - \int \frac{\rho_A(r)}{\rho_{promolecules}(r)} \rho_{molecules}(r) dr$$

(4)

$$Q_A^{VDD} = -\int \left[\rho_{molecules}(r) - \rho_{promolecules}(r)\right] dr$$

(5)

More data are better to describe the comparison and conclusion in the experiments, and based on that, we have performed the zero deferential overlap (ZDO) atomic charges analysis. ZDO population analysis is based on the Hückel Theory that takes a linear combination of atomic orbitals-molecular orbital method. Here the multiplication of differential atomic orbital between two atoms is set to zero and further performs the integration of differential atomic orbital of all the consecutive bonds that are formed by two atoms in the molecules, these results considered the uniform charge sphere and the rest parameterized [28].

In Figures 3 and 4. the comparison of atomic charges are plotted using Mulliken, zero deferential overlaps (ZDO), Hirshfeld, and Vornoi population analysis of Glc-Arg and Glc-Cys, respectively. From Figure 2. while considering the position of specific atoms in the molecules of Glc-Arg and Glc-Cys, the atomic charges of each atom in the molecules were analyzed and described in the Supplementary Information.

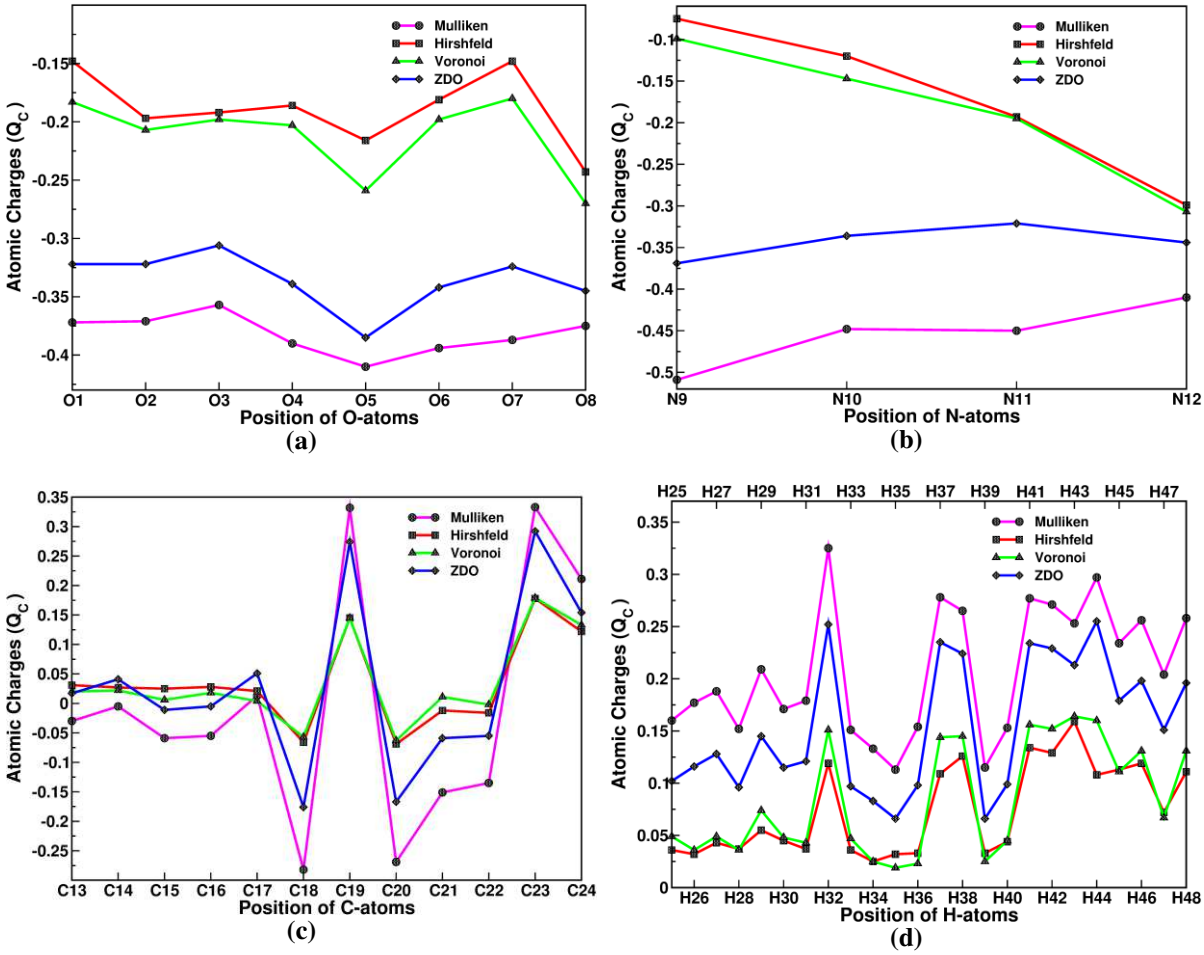

Figure 3: Mulliken, Hirshfeld, Vornoi and ZDO population analysis of Glc-arg atom (a) Oxygen positioned atoms (b) Nitrogen positioned atoms (c) Carbon positioned atoms (d) Hydrogen positioned atoms

The atomic charges of Oxygen(O) atoms and Nitrogen(N) atoms present in the Glc-Arg are given in Figure 3(a,b). , which is in the range of -0.125e to -0.425e and -0.075e to -0.055e, respectively. Both the O and N atoms behave as electron-donating atoms in the molecules, which means when any electrophilic chemical species interact with such atoms, the motion of charge transfer between them can be seen. From Figure 3(c). we can conclude that the Carbon(C) atoms present in Glc-Arg show both positive and negative atomic charge distributions, within the range of -0.300e to 0.350e. The negatively charged C atoms are not good donors as compared to the O and N atoms present in the molecules due to their low magnitude of atomic charges. However, the C19, C23, and C24 show a high magnitude of atomic charges when compared with other C-atoms in the Glc-Arg. These C-atoms readily accept an electron from foreign molecules. The atomic-charge values for Hydrogen atoms (H) in the molecule are represented in Figure 3(d), which varies from 0.025e to 0.325e. All the H-atoms show a positive atomic-charge distribution, which means when any foreign nucleophilic chemical species interacts with these H-atoms, there is a possibility of bond formation or transfer of charge between them.

In Figure 4(a), the population analysis of Sulphur(N), Oxygen(O), and Nitrogen(N) atoms present in the Glc-Cys exhibits variation from -0.025e to -0.425e, where the negative charge distribution show the tendency to donate electrons to the electrophilic chemical species. The Glc-Cys also consists of Carbon(C) and Hydrogens(H) atoms, and their population analysis are given in Figure 4(b,c). The position of C16, C18, and all H-atoms show positive atomic charges that behave as electron-accepting atoms and are considered to be good sites for nucleophilic chemical species interaction.

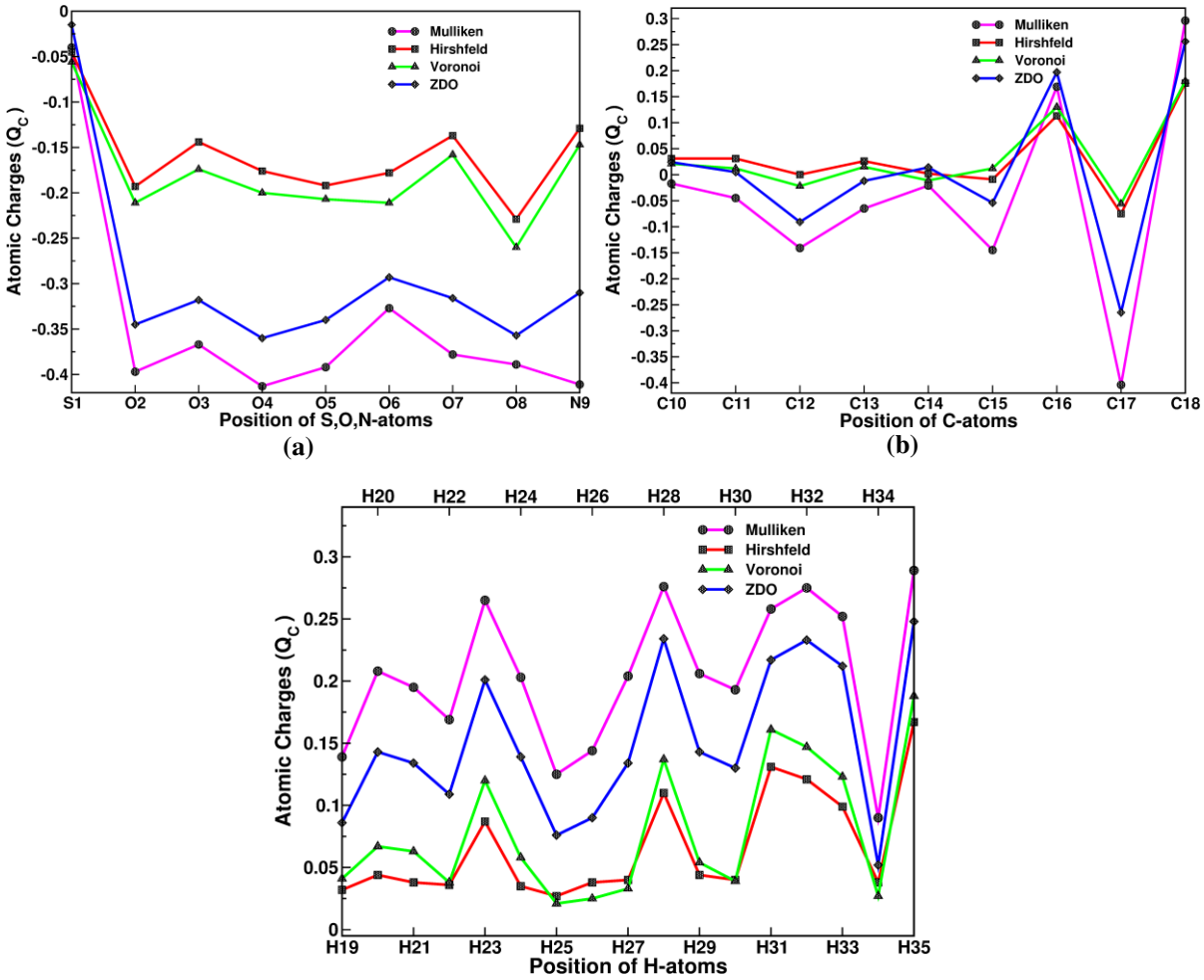

Figure 4: Mulliken, Hirshfeld, Vornoi and ZDO population analysis of Glc-cys atom (a) Sulphur, Oxygen, Nitrogen positioned atoms (b) Carbon positioned atoms (c) Hydrogen positioned atoms

3.3 Bond Length and Bond Angle

The optimized average bond length between all the possible bonds in the structures of Glc-Arg and Glc-Cys are outlined in Table 2. The bond length between the atoms of C-H, C=O, N-H, and O-H do not vary in Glc-Arg and Glc-Cys molecules. The net difference in bond length between C and O atoms are 0.18 Å and 0.20 Å in the molecules of Glc-Arg and Glc-Cys, respectively, and that is due to an increase in bond order. The bond length between C-S is 1.84 Å, the highest bond length present in Glc-Cys, which is due to an increase in the size of the atom and the distance from the internuclear axis. The bond distance between each atom present in Glc-Arg and Glc-Cys molecules is listed in the Supplementary Information.

Table 2: Optimize Bond Length Pair

Molecules	Element Pair	Average Bond Length (Å)
Glucose-Arginine (Glc-arg)	C—H C—N C—O, C=O N—H O—H	1.12 1.39 1.42,1.24 1.03 0.99
Glucose-Cystene (Glc-cys)	C—H C—N C—O, C=O C—S N—H O—H S—H	1.12 1.46 1.44, 1.24 1.84 1.03 0.99 1.38

3.4 Charge Density Plot

The plot of charge density exhibits the distribution of electric charge present in the atoms of the molecule, which helps to predict the type of bond present between atoms. These chemical bonds arrangements are based on the formation of concentric circles (unequal sharing) and the dumbbell shapes (equal sharing) around atoms that tell the nature of the bond that are ionic and covalent, respectively [29]. Molecules of Glc-Arg and Glc-Cys have a V-shaped non-planar structure, and the plotting of charge density is only possible through the 2D plane, due to this reason, we have aligned the molecules in the XZ-plane, and the charge density distribution is calculated along (010) plane.

In Figure 5(a&b), the charge density plot, and their scale with the color code are represented at the top-right and top-left of Glc-Arg and Glc-Cys molecules, respectively. In Glc-Arg and Glc-Cys molecules, the D-glucose molecule chemically makes the bond with N-atoms present in Arginine and Cysteine, forming a C-N bond. From Figure 5(a&b), it can be analyzed that the bond between C-N is partially covalent and ionic, which is due to the concentric circles formed around the N-atoms and deformed dumb-bell shapes around the bond formed, and from the charge scale, we can observe a higher electron density at the inner-most region (magenta) and the lowest electron density at the outermost region (cyan and yellow), this is because the charge density near the atoms is denser and with the increase in distance, it gets reduced.

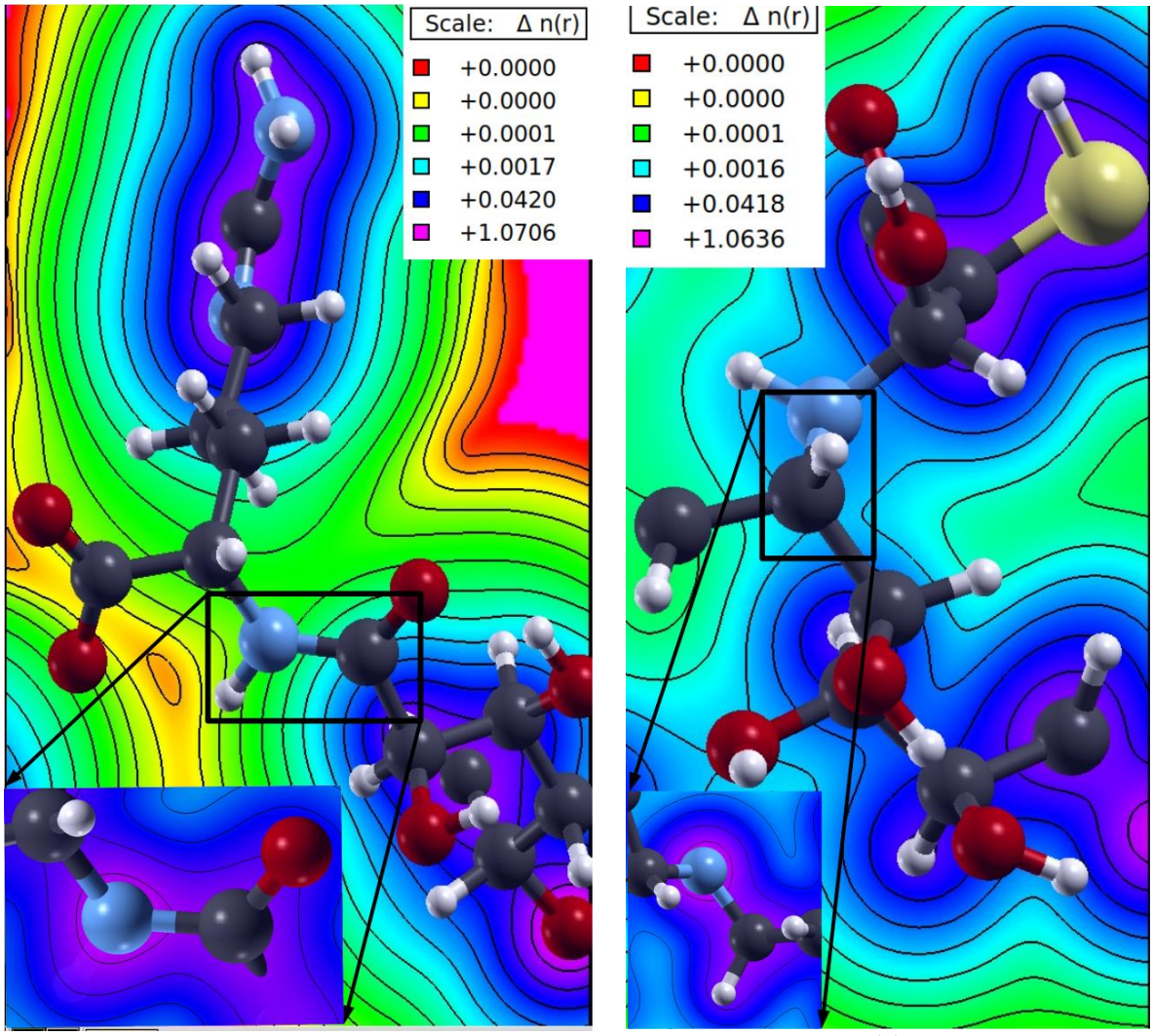

Figure 5: Charge density plot of (a) Glc-arg and (b) Glc-cys

3.5 Electronic properties analysis

The study of Density of States (DOS) plots gives information about the presence of electrons, in their available energy states that are formed due to the overlapping of their atomic orbitals energy bands. DOS plots help to determine the energy of the Highest Occupied Molecular Orbital (HOMO)and Lowest Unoccupied Molecular

Orbitals (LUMO) present in the molecule [30]. In Figure 6(a). the DOS plots of Glc-Arg and Glc-Cys are plotted in which the Y-axis denoted the concentration of electrons, and the X-axis represented the available energy levels of molecular orbitals. The left and right regions of the Fermi level are represented as valence band and conduction band, respectively. The molecular orbital energy gap is the difference in the energy level of HOMO and LUMO that results in the gain or loss of energy when electron donor-acceptor transfer takes place in the system. However, the molecular orbital energy gap (Eorbital) between HOMO-LUMO orbitals tells us the chemical reactivity and the kinetic stability of the molecule.

The energy of HOMO and LUMO are calculated from the DOS plot, and the energy at which the first highest peak formed in the valence band is known as E_{HOMO}, whereas E_{LUMO} is in the conduction band.

Table 3: Energy level of orbitals

Molecules	Fermi level	E_{HOMO}	E_{LUMO}	$E_{orbital}$
Glc-Arg	-3.9832	-5.6290	-2.0272	±3.6018
Glc-Cys	-4.3956	-5.9814	-2.8999	±3.0815

In Table 3. the energy levels of HOMO(E_{HOMO}), LUMO(E_{LUMO}), and their energy gap(E) are given, in which the Fermi level is -3.9832 for Glc-Arg and -4.3956 for Glc-Cys. Observations show that when the molecule's orbital energy gap is narrow, chemical reactivity increases and kinetic stability decreases when compared to molecules with a large orbital energy gap. After analyzing the bandgap of Glc- Arg, and Glc-Cys, it concluded that both molecules behave like an insulator due to the large gap in their energy levels.

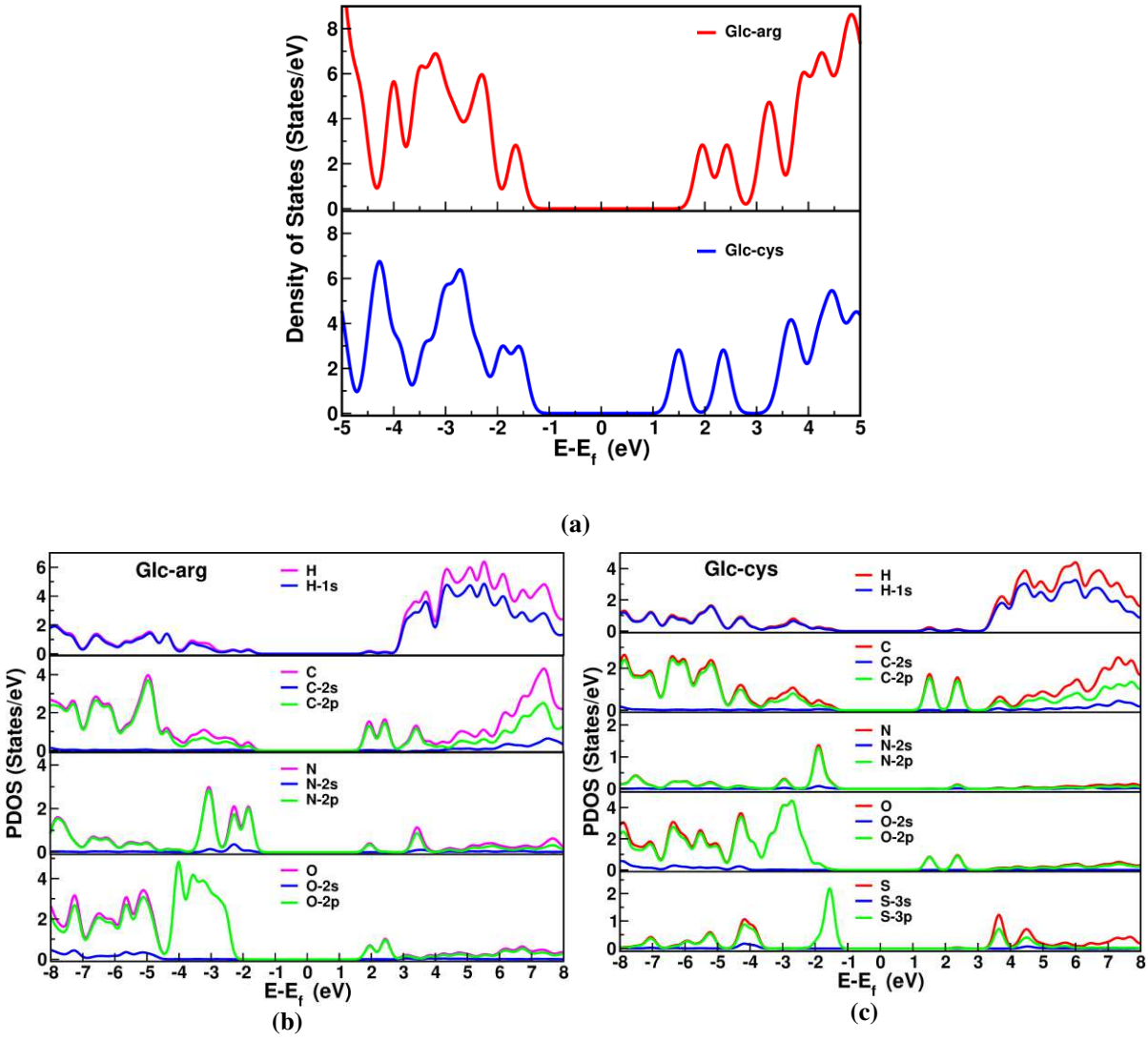

Figure 6: (a) Density of states plot of Glc-arg and Glc-cys Projected Density of States of (b) Glc-arg (c) Glc-cys

The formation of molecules involves the energy participation, orientation, and alignment of constituent elements that play an essential role in their structural and physical properties. In Glc-Arg and Glc-Cys molecules, to understand the contribution of orbitals of each specific element at an obtainable energy level of valence and conduction band, we have used their Projected Density of States (PDOS) plots. In Figure 6(b,c). PDOS plots of Glc-Arg and Glc-Cys molecules are represented in which the C, N, O, and S atoms showing the overall contribution orbitals where particularly p-orbital almost overlap both, in valence and conduction bands, which means that the p-orbital is dominant over s-orbital. But in the H atom, the s-orbital is dominant and overlaps in Glc-Cys and Glc-Arg molecules due to the unavailability of p-orbital in n=1 energy level.

3.6 Chemical Reactivity

Molecular orbitals play a vital role in the electronic, chemical, and structural properties of molecules, and to understand the competence of molecular orbital energy of Glc-Agr and Glc-Cys molecules, we should know the ionization potential (energy required to remove an electron from the outermost orbital of an atom or a molecule) and electron affinity (energy change due to the addition of an electron in the orbital of an atom). By using Koopmans' theorem, we can find the ionization potential (ı) and electron affinity (A) energy, according to which in closed-shell Hartree-Fock theory, the first ionization energy is equal to the negative of the energy of HOMO, and A is equal to the eigenvalue of LUMO with no switch in sign, present in Glc-Arg and Glc-Cys molecules, respectively [31]. These ı and A helps to determine the Global reactivity criteria in initial electron distribution such as Chemical Potential (μ), Global Hardness (η), Global Softness(ζ), also Electronegativity (χ) and Electrophilicity Index (ω) of molecules by equations recommended by Iczkowski and Margrave and Maynard, Parr based on their Lagrange multiplier normalization of density and the finite differences approximations [32].

These ı and A helps to determine the Global reactivity indices such as Electronegativity (χ), Global Hardness(η), Global Softness(ζ), Electrophilicity Index (ω) of molecules by equations recommended by Maynard and Parr, based on their Lagrange multiplier normalization of density and the finite differences approximations . However, the Electrodonating Power (ω-), Electroaccepting Power (ω+) and Net Electrophilicity (Δω) can be calculated by the equation derived by Gazquez, assuming global hardness is equal in donor and acceptor region both, which is equal to the difference in Chemical Potential for electron donation (μ-) and Chemical Potential for electron acceptance (μ+), that uses the quadratic interpolation and Taylor series for the energy functional [33].

The chemical reactivity indices of Glc-Arg and Glc-Cys molecules are tabulated in Table 4. prepared with the help of their energy of HOMO and LUMO given in Table 3. Glc-Arg behaves as a superior electron donor because its ionization potential is 6 % lower than the Glc-Cys, and shows high polarizability and chemical reactivity. But, the electron affinity of Glc-Cys is 30% larger than Glc-Arg, which results in Glc-Cys having dominant behavior in accepting an electron in LUMO. The chemical potential tells us the threshold intrinsic energy of the electron to escape from HOMO to LUMO energy level for charge transfer, and the Glc-Arg molecule shows the higher chemical potential. The hardness and softness of molecules can be determined when there is a large difference in the energy level of HOMO-LUMO that results in hard molecules which inhibit the charge transfer whereas, the small HOMO-LUMO gap results in soft molecules. Glc-Arg behaves as the hard molecules, and Glc-Cys act as the soft molecules.

The charge transfer from the surrounding electrophilic or nucleophilic chemical species creates a change in the total energy of the molecular orbitals, and these stabilization energy measurements result in the Electrophilicity Index of a molecule. Glc-Cys having 36 % and 14 % higher Electrophilicity Index and electronegativity(tendency to attract electrons) respectively results in high toxicity that is due to the lower nucleophilic atoms present in Glc-Cys comparable to Glc-Arg.

Chemical Potential for Electron Donation (μ-) and Electron Acceptance (μ+) can be calculated using the differential equation, on the Chemical potential of the system in the range from the charge donation region to charge acceptance region, which is the left and right derivatives when the charge transfer occurs. The determination of these two properties helps us to calculate the Electrodonating Power and Electroaccepting Power. Glc-Cys shows the higher Electroaccepting power that explains its high capability of accepting charge, although the Electrodonating power of Glc-Arg is higher, and it behaves like a good electron donor. The net

electrophilicity of Glc-Cys is 35 % higher than Glc-Arg, which shows it has higher average electrophilic power, and this helps to measure the electron accepting-donating strength of molecules.

Table 4: Glocal Chemical Reactivity indices

Chemical Properties	Formula	Glc-Arg	Glc-Cys
Ionization Potential (eV)	$I = -E_{HOMO}$	5.6290	5.9814
Electron Affinity (eV)	$A = -E_{LUMO}$	2.0272	2.8999
Chemical Potential (eV)	$\mu = -\frac{1}{2}(I + A)$	-3.8281	-4.4406
Donation Chemical Potential (eV)	$-\frac{1}{4}(3I + A)$ $\mu^{-}=$	-4.7286	-5.2110
Acceptance Chemical Potential (eV)	$-\frac{1}{4}(I + 3A)$ $\mu^{+}=$	-2.9277	-3.6703
Electronegativity (eV)	$\chi = -\mu = \frac{1}{2}(I + A)$	3.8281	4.4406
Global Hardness (eV)	$\eta = \frac{I - A}{2}$	1.8009	1.5408
Global Softness $(eV)^{-1}$	$\zeta = \frac{1}{2\eta}$	0.2776	0.3245
Electrophilicity Index (eV)	$\omega = \frac{(\mu)^2}{2\eta}$	4.0687	6.3992
Electrodonating Power (eV)	$\omega^{-}=\frac{(3I+A)^2}{16(I-A)}$	6.2078	8.8121
Electroaccepting Power (eV)	$\omega^{+}=\frac{(I+3A)^2}{16(I-A)}$	2.3797	4.3714
Net Electrophilicity (eV)	$\Delta\omega=\omega^{+}-(\omega^{-})$	8.5875	13.1835

The surface calculations help to determine the reactive sites of a molecule for nucleophilic and electrophilic interactions. We have performed the molecular electrostatic potential (MEP) and HOMO-LUMO surface calculations. Molecular electrostatic potential tells us the required potential for Vander Waal interaction or chemical bond formation in the different areas of molecules by foreign electrophilic chemical species. The HOMO-LUMO surface calculation signifies that when a bond is formed due to the interaction of atomic orbitals of constituent elements, a region is found, showing the highest occupied and lowest unoccupied molecular orbitals of the molecules are present [34]. Therefore it is the first most effective reaction site, supporting the nucleophilic and electrophilic attack.

3.7 Electrostatic potentials Map and HOMO – LUMO surface

In Figure 7a. the MEP surface of Glc-Arg and Glc-Cys have presented in which the color code and quantitative scale are represented in the left side of the picture that is in the Atomic unit (a.u.).

With an increase in the electrostatic potential, different colors have been used at the surface of molecules, like the magenta color represents the highest electrophilic repel region and red color shows the high negative electrostatic potential that shows the finest site for the electrophilic attack. In Figure 7a., we can analyze that in both, Glc-Arg and Glc-Cys molecules, the position of all O-atoms represents negative electrostatic potential, and all H-atoms show positive electrostatic potential. The green, blue, and cyan colors are have been observed around C and N atoms that represent the midst electrostatic potential region.

Orbital energy difference and surface calculations between HOMO-LUMO of Glc-Arg and Glc-Cys molecules have been presented in Figure 7b. in which red color represents the increase in electron density and blue color represents the decrease in electron density. The HOMO and LUMO region shows the instability region of the molecules due to the tendency to donate and accept electrons by the molecular orbital. In both, the molecules of Glc-Agr and Glc-Cys, the region of d-glucose does not show any HOMO-LUMO surface that means this region is the stable region of the molecules. The orbital energy difference in Glc-Arg is 3.6018 eV and 3.0815 eV for Glc-Cys. In Glc-Arg, the lower moieties of arginine represent the HOMO region, and on the other hand, the chemical bond formed between Glc and Arg shows the LUMO region.

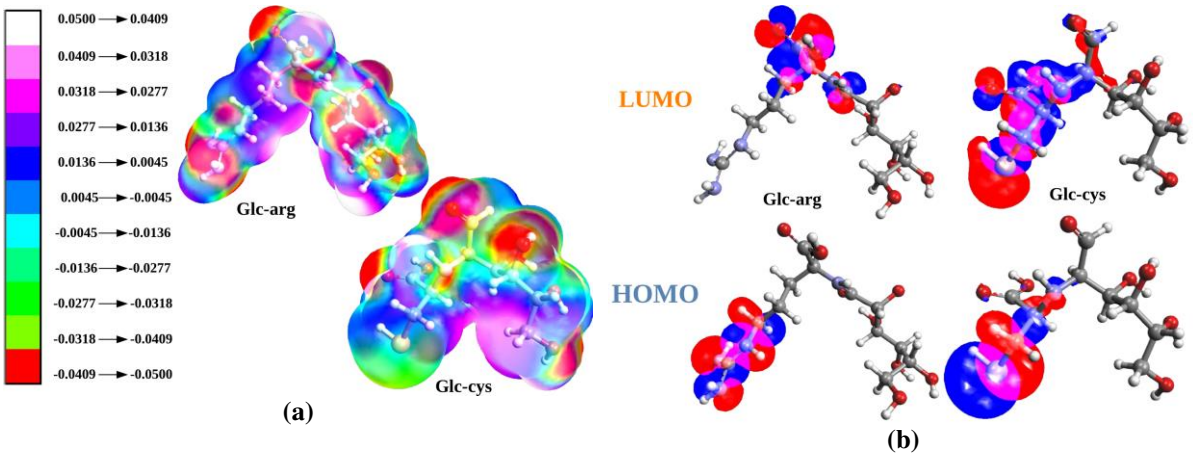

Figure 7: (a) Electrostatic Potential map of Glc-arg and Glc-cys molecules (b) HOMO-LUMO surface of Glc-arg and Glc-cys.

Glc-Arg and Glc-Cys molecules, if any force has been exerted from external molecules or materials and to know their strength, mechanical stability, and elasticity of the molecules, we perform the tensile stress-strain calculations. The mechanical stability of molecules can be determined by their Energy vs Strain plotting, where the strain is applied in molecules with a 1% regular variation along the x-axis, y-axis, and z-axis of the lattice box.

3.8 Mechanical Strength

In Figure 8(a,b). calculations of mechanical stability are represented for compression (decrease in length) and elongation (increase in length) when a strain is applied in Glc-Arg and Glc-Cys molecules along the different planes. The alignment and arrangement of all atoms of Glc-Arg and Glc-Cys molecules are in the XZ-plane, being perpendicular to Y-axis outwardly, which is shown in Figure 2. When we apply strain on Glc-Arg and Glc-Cys molecules towards the y-axis(XZ-plane) and z-axis (XY-plane), we can see an insignificant change in the total energy (ETotal), which indicates that along these axes, the molecules are mechanically stable, and elongation-compression does not occur. While along the x-axis (YZ-plane) total energy of molecules increases during compression due to the V-shaped area occupied by the lattice, whereas elongation increases gradually. To balance the total energy calculation, we have set the range at least -0.05 % for compression (on negative x region), and on the other hand, +0.15 % for elongation (on positive x-region). In Glc-Arg and Glc-Cys molecules, the total energy changes during compression, which is due to the decrease in the internuclear distance, and this affects the exchange-correlation energy.

The tensile stress of Glc-Arg and Glc-Cys molecules are plotted in Figure 8(c). by applying a strain along the x-axis just because we analyzed the acceptable change in total energy.

$$\sigma = \frac{1}{\Omega(\epsilon)} \frac{\partial E}{\partial \epsilon} \tag{6}$$

Equation 6. is used to calculate the tensile stress along the x-axis where σ is tensile stress, E is the total energy, and Ω (ε) is the volume at given strain (ε) [35].

From Figure 8(c). we can analyze that when we increase the strain in the compression region, the tensile stress increases suddenly, and the Glc-Arg molecule shows comparatively high tensile stress than the Glc-Cys

molecule, which is due to its higher net change in energy (dE) and volume. In the elongation region, we can analyze tensile stress-strain based on three parameters, including the linear relation between stress-strain(which follows Hooks law), maximum threshold elasticity limit, and occurrence of plasticity behavior. Glc-Arg and Glc-Cys molecules follow the Hooks law and give a linear proportional correlation till 0.01 % strain is applied, which is shown in the subplot of Figure 8(c). According to our analysis, 0.04 % and 0.06 % is the maximum elastic limit point, at which the molecules have 0.000376 eV/ $Å^3$ and 0.000731eV/$Å^3$ tensile stress, and before this strain it having potential to regain their shape and shows elasticity behavior in Glc-Arg and Glc-Cys, respectively. After applying threshold strain value, there are no hopes for elasticity to occur, and plasticity behavior arises. The tensile stress remains almost consistent in the duration of the remaining deformation stage till fracture occurred.

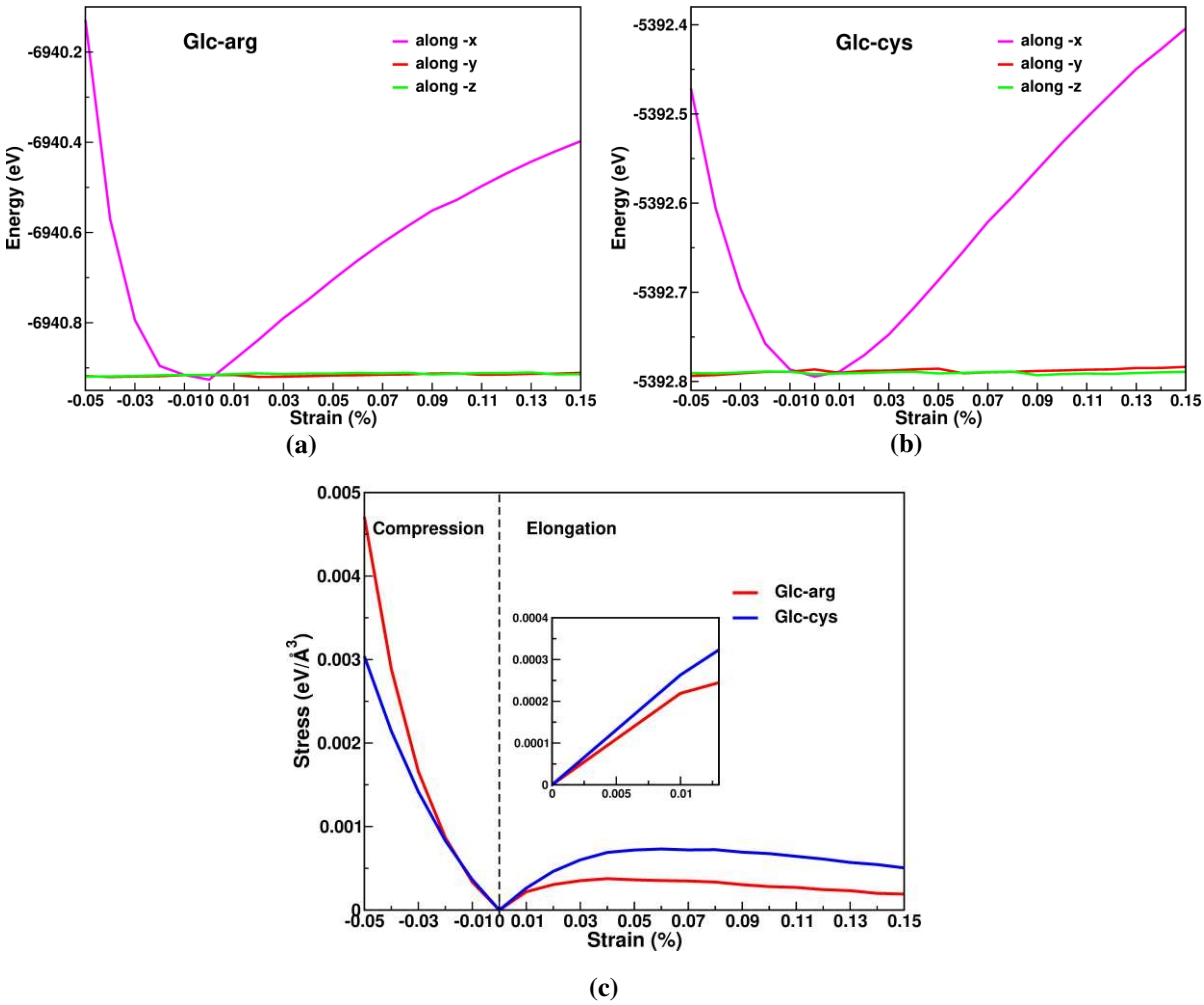

Figure 8: Energy vs strain along x, y and z axes of (a) Glc-arg and (b) Glc-cys Stress vs Strain

3.9 Transport properties analysis

Studying the details about the Electron transport of the Glc-Arg and Glc-Cys molecules gives us information about the scattering state, transmission coefficient, and IV characteristics. For transport calculation, we have to design a cell that is divided into three parts left: electrode | scattering region | right electrode, connected in a sequence. The Graphene sheet of 88 atoms in the left-right part of the cell is used as electrodes for the transport analysis, which is periodic in arrangement, whereas the contact active material is non-periodic. When we attach the left and right electrodes to nanostructured molecules of Glc-Arg and Glc-Cys, their energy levels get shifted (Figure 9.), comparatively before the connection with the electrode as shown in Figure 6, representing their HOMO-LUMO gap. The molecular orbitals are present in the molecules, and each orbital has a different level of energy and is categorized based on its occupancy in two regions, which are valence band, and conduction band. When the source electrons from the electrode interact and transfer the charge between these energy level orbitals (nanostructure material), then the concentration of electrons varies and affects the energy levels of density of states (DOS). In forward biased, the left electrode behaves as a source(electron incident), and on the other hand, the right electrode acts like a drain(electron transmission) [36]. The transmission coefficient is the relation

between the transmitted power of the electron from available energy levels in Glc-Arg and Glc-Cys molecules to the incident power that comes from contact electrodes in the form of coupling functions, ranging from 0 to 1.

The transmission coefficient between left and right electrodes is given by:

$$T(E,V) = Tr[\Gamma_L(V)G(E,V)\Gamma_R(V)G*(E,V)] \quad (7)$$

In equation 7, the term G and G* are the retarded, and advanced Green functions of the transmission region, and here Γ L and Γ R are the coupling functions of the left and right electrodes.

In Figure 9(a,b), the transmission coefficient VS energy level graph represents the Glc-Arg and Glc-Cys molecules, respectively. From Figure 9(a,b). the transmission curves at the voltage supply of 0.4 V, 1.0 V, and 1.4 V are exhibited, and in all these cases, there is a large gap between the valence and conducting region for the charge transfer. But, with an increase in the supply of the voltage, the transmission spectra move closer, and slightly reduce the gap. It has been observed that the Glc-Arg molecule shows high dense transmission spectra, as compared to the Glc-Cys molecule, with the energy level range of -4.0 to -9.0 eV.

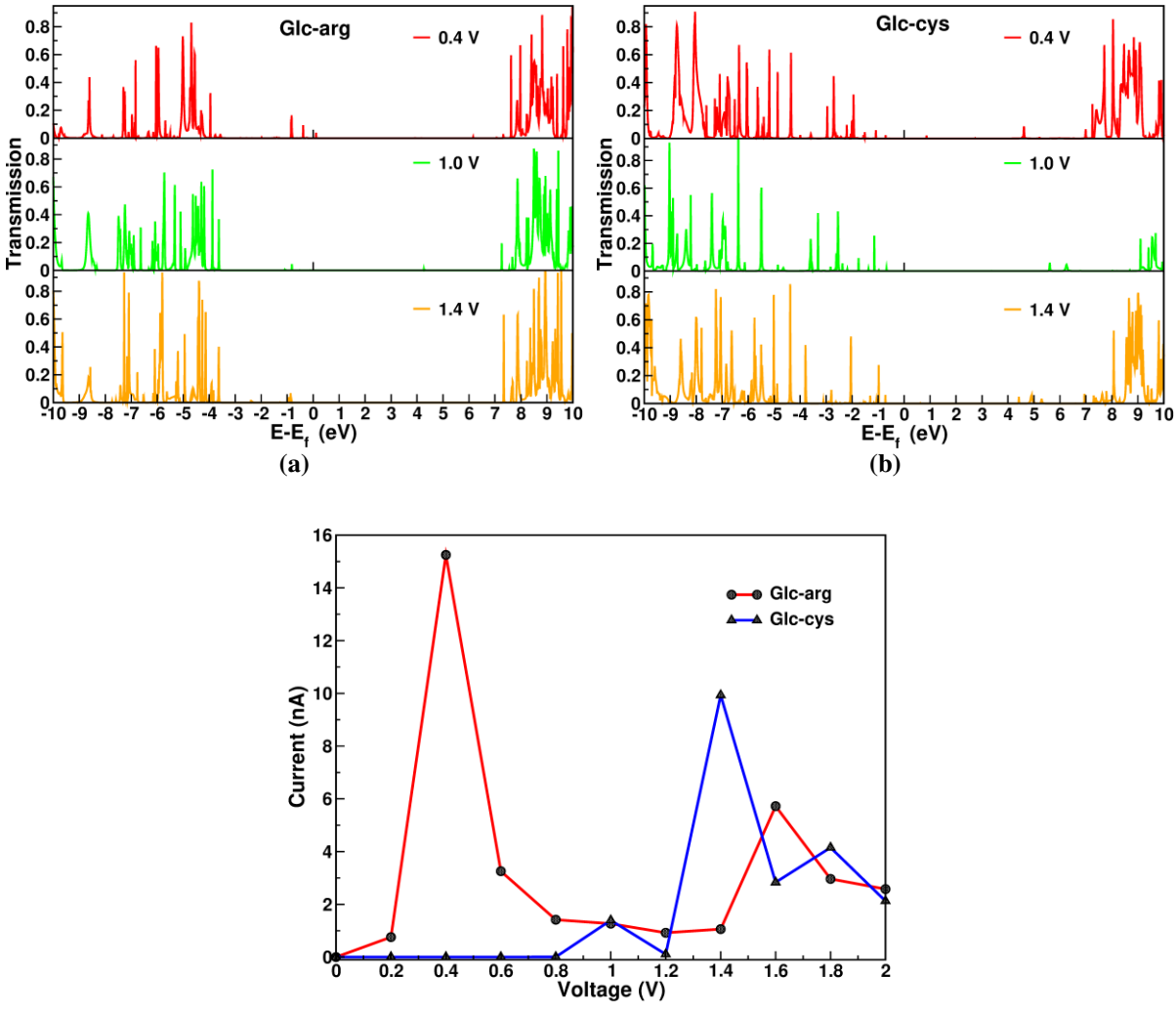

Figure 9: Transmission probability of (a) Glc-arg (b) Glc-cys in 0.4 V, 1.0 V and 1.4 V (c) IV-characteristics of Glc-arg and Glc-cys molecules

In the Landauer–Butiker formula, equation 8, {f(E-μL)-f(E-μR)} represent a distribution function where f is the Fermi–Dirac function, μL and μR represent electrochemical potentials of left and right electrodes, respectively. 2e/h is known as quantum conductance, where h is the Planck's constant and e is the charge of an electron. T(E, V) is a function of bias voltage (V) with energy (E) transmitting through the device, and it shows the transmission coefficient of the charge carrier [37].

$$I(V) = \frac{2e}{h} \int [f(E - \mu L) - f(E - \mu R)]\, T(E, V) dE$$
(8)

The IV characteristics of Glc-Arg and Glc-Cys molecules are analyzed only in the positive bias, as shown in Figure 9(c). , since on applying negative bias, we got the value of the current in the range of pico Ampere, whereas it was in the range of nano Ampere in the case of positive bias. This large difference in the output current is due to the occupied or HOMO region, which was under consideration in negative bias, although in the positive bias, it probed unoccupied or LUMO region of molecules, and the strength of coupling function of the left electrode and right electrode also affect the output current.

From Figure 9(c). it was observed that at 1.0 V and 2.0 V supplied voltage in Glc-Arg and Glc-Cys molecules, there is an almost equal output current. In Glc-Arg, two higher peaks are formed at 0.4 V and 1.6 V with current values 15 nA and 6 nA, respectively. However, on applying a voltage of 1.4 V and 1.8 V in Glc-Cys, we get the higher peaks with the values of current 10 nA and 4 nA, respectively. It was observed that when we increased the applied voltage, the output current variation was uncertain but their measurement scale was always in nA, and it is due to variation in transmission coefficient calculation, caused through scattering region and negative differential resistance (NDR), that is the cause of misalignment in the energy levels of electrodes and nanostructured molecular orbitals with the increase in bias voltage.

4. Conclusion

In this work, the Maillard reaction helps to the formation of Glc-arg and Glc-cys molecules are investigated using density functional theory. SIESTA software is used for the implementation of density functional theory and explored the structural, electronic, chemical reactivity, mechanical stress and transport properties. The orbital energy gap of Glc-arg and Glc-cys molecules is 3.6018 and 3.0815, it concluded that both molecules behave as insulators. The Charge density plot shows that the bond formation between the D-glucose with arginine and cysteine is in between s-p orbital, it is partially covalent and ionic. The Electrostatic potential map and HOMO-LUMO surface of Glc-arg and Glc-cys are investigated in which the dominant reaction regions shows the prime arginine and cysteine of molecules. The chemical reactivity of Glc-arg molecules is high with corresponding to the secretion of insulin in diabetic treatment, in contrast to Glc-cys molecules. The tensile strength of both Glc-arg and Glc-cys are slightly different in the value and the Energy vs Stress plot shows the variation along X-axis only. The IV-characteristics of Glc-arg and Glc-cys molecules is the trivial and efficient value of current in nano-Ampere scale with a voltage applied 0-2 V.

Acknowledgement

The authors are grateful to the management of Shri Shankaracharya Technical Campus in Bhilai, especially Dr. B.Keshav Rao, for their assistance with this study. The authors would like to express their gratitude to Prof. Ravindra Pandey of Michigan Technological University for his helpful advice. The authors would like to express their gratitude for Dr. Laxmikant Chaware's tremendous help.

Declarations of Interest

Funding:

The authors received no financial support for the research, authorship, and/or publication of this article.

Conflicts of interest:

The authors declare that they have no known competing financial interests or personal relationships that could have appeared to influence the work reported in this paper. I declare that this research work is not communicated anywhere, it is solely communicated to this journal, and the conclusions are the outcomes of our findings. This manuscript has not been submitted to, nor is under review at, another journal or other publishing venue.

Availability of data and material:

All of the data in this study was created independently, and not a single piece of information was copied from another source.

Code availability:

Codes are available in this work is self makes by using Spanish Initiative for Electronic Simulations with Thousands of Atoms (SIESTA) software.

Authors' contributions:

All authors have contributed differently to complete this research work.

Shreya Tiwary – Writing and Reading

Hemant Kumar – Conceived and designed the analysis, analysis or interpretation, Performed the analysis, Wrote the paper, Collected the data

Mohan L. Verma – writing and approval of the final version

Deepti Pateria - drafting the article or revising it critically for important intellectual content

References

1. Lea Lojkova, Valerie Vranová, Pavel Formánek, Ida Drápelová, Martin Brtnicky, Rahul Datta, Enantiomers of Carbohydrates and Their Role in Ecosystem Interactions: A Review, Symmetry 2020, 12, 470; doi:10.3390/sym12030470
2. João F. Lopes; Elvira M.S.M. Gaspar (2008). *Simultaneous chromatographic separation of enantiomers, anomers and structural isomers of some biologically relevant monosaccharides. , 1188(1), 34 42.* doi:10.1016/j.chroma.2007.12.016
3. Stefan-van Staden, Raluca-Ioana; Mitrofan, Grigorina (2018). *Molecular enantiorecognition of <scp>l</scp> -glucose and <scp>d</scp> -glucose in whole blood samples. Chirality,* doi:10.1002/chir.22843
4. Tessari, Paolo; Lante, Anna; Mosca, Giuliano (2016). *Essential amino acids: master regulators of nutrition and environmental footprint?. Scientific Reports, 6(), 26074–.* doi:10.1038/srep26074
5. Yang, Qingqing; Zhao, Dongsheng; Liu, Qiaoquan (2020). *Connections Between Amino Acid Metabolisms in Plants: Lysine as an Example. Frontiers in Plant Science, 11(), 928–* . doi:10.3389/fpls.2020.00928
6. Rose, (2019). *Amino Acid Nutrition and Metabolism in Health and Disease. Nutrients, 11(11), 2623–* . doi:10.3390/nu11112623
7. Kohlmeier, Martin (2015). *Nutrient Metabolism || Amino Acids and Nitrogen Compounds. , (), 265–477.* doi:10.1016/B978-0-12-387784-0.00008-0
8. Staden, Raluca-Ioana Stefan-van; Popa-Tudor, Ioana; Ionescu-Tirgoviste, Constantin; Stoica, Roxana-Adriana; Magerusan, Lidia (2019). *Molecular Enantiorecognition of D- and L-Glucose in Urine and Whole Blood Samples. Journal of The Electrochemical Society, 166(9), B3109–B3115.* doi:10.1149/2.0211909jes
9. Asiimwe, Debrah; Mauti, Godfrey O.; Kiconco, Ritah (2020). *Prevalence and Risk Factors Associated with Type 2 Diabetes in Elderly Patients Aged 45-80 Years at Kanungu District. Journal of Diabetes Research, 2020(), 1–5.* doi:10.1155/2020/5152146
10. Chiang, Jane L.; Kirkman, M. Sue; Laffel, Lori M.B.; Peters, Anne L. (2014). *Type 1 Diabetes Through the Life Span: A Position Statement of the American Diabetes Association. Diabetes Care, 37(7), 2034–2054.* doi:10.2337/dc14-1140
11. Olokoba, Abdulfatai B.; Obateru, Olusegun A.; Olokoba, Lateefat B. (2012). *Type 2 Diabetes Mellitus: A Review of Current Trends. Oman Medical Journal, 27(4), 269–273.* doi:10.5001/omj.2012.68
12. Lund, Marianne N.; Ray, Colin (2017). Control of Maillard reactions in foods: strategies and chemical mechanisms. Journal of Agricultural and Food Chemistry, (), acs.jafc.7b00882–. doi:10.1021/acs.jafc.7b00882
13. Hemmler, Daniel; Roullier-Gall, Chloé; Marshall, James W.; Rychlik, Michael; Taylor, Andrew J.; Schmitt-Kopplin, Philippe (2018). *Insights into the Chemistry of Non-Enzymatic Browning Reactions in Different Ribose-Amino Acid Model Systems. Scientific Reports, 8(1), 16879–.* doi:10.1038/s41598-018-34335-5
14. Lucotti, P.; Setola, E.; Monti, L. D.; Galluccio, E.; Costa, S.; Sandoli, E. P.; Fermo, I.; Rabaiotti, G.; Gatti, R.; Piatti, P. (2006). *Beneficial effects of a long-term oral L-arginine treatment added to a hypocaloric diet and exercise training program in obese, insulin-resistant type 2 diabetic patients. AJP: Endocrinology and Metabolism, 291(5), E906–E912.* doi:10.1152/ajpendo.00002.2006
15. Sogut, Ece; Ertekin Filiz, Bilge; Seydim, Atif Can (2020). *A model system based on glucoseâ arginine to monitor the properties of Maillard reaction products. Journal of Food Science and Technology, (), –* . doi:10.1007/s13197-020-04615-y

16. Sushil K. Jain; Thirunavukkarasu Velusamy; Jennifer L. Croad; Justin L. Rains; Rebeca Bull (2009). *l-Cysteine supplementation lowers blood glucose, glycated hemoglobin, CRP, MCP-1, and oxidative stress and inhibits NF-κB activation in the livers of Zucker diabetic rats. , 46(12), 1633–1638.* doi:10.1016/j.freeradbiomed.2009.03.014
17. Kaneko, Y.; Kimura, Y.; Kimura, H.; Niki, I. (2006). *L-Cysteine Inhibits Insulin Release From the Pancreatic -Cell: Possible Involvement of Metabolic Production of Hydrogen Sulfide, a Novel Gasotransmitter. Diabetes, 55(5), 1391–1397.* doi:10.2337/db05-1082
18. Artacho, Emilio; Gale, Julian D; Soler, José M; García, Alberto; Junquera, Javier; Ordejón, Pablo; Sánchez-Portal, Daniel (2002). *The SIESTA method for ab initio order-N materials simulation. , 14(11), 2745–2779.* doi:10.1088/0953-8984/14/11/302
19. http://www.uam.es/siesta.
20. Perdew, John P.; Burke, Kieron; Ernzerhof, Matthias (1996). *Generalized Gradient Approximation Made Simple. , 77(18), 3865–3868.* doi:10.1103/physrevlett.77.3865
21. Ednara Joice Braga 1 , Brena Tabosa Corpe 1 , Márcia Machado Marinho 2 , Emmanuel Silva Marinho, Molecular electrostatic potential surface, HOMO–LUMO, and computational analysis of synthetic drug Rilpivirine, International Journal of Scientific & Engineering Research, Volume 7, Issue 7, July-2016, ISSN 2229-5518.
22. KURT STOKBRO; JEREMY TAYLOR; MADS BRANDBYGE; PABLO ORDEJÓN (2003). *TranSIESTA: A Spice for Molecular Electronics. , 1006(none), 212–226.* doi:10.1196/annals.1292.014
23. Banger, Suman; Nayak, Vikas; Verma, U. P. (2017). *AIP Conference Proceedings [Author(s) DAE SOLID STATE PHYSICS SYMPOSIUM 2016 - Bhubaneswar, Odisha, India (26–30 December 2016)] - Cohesive energy of KH+nH (n=0, 2, 6, 8): A DFT study. , 1832(), 140003–.* doi:10.1063/1.4980785
24. Mole, Susan J.; Zhou, Xuefeng; Liu, Ruifeng (1996). *Density Functional Theory (DFT) Study of Enthalpy of Formation. 1. Consistency of DFT Energies and Atom Equivalents for Converting DFT Energies into Enthalpies of Formation. The Journal of Physical Chemistry, 100(35), 14665–14671.* doi:10.1021/jp960801h
25. Pokharia, Sandeep; Joshi, Rachana; Pokharia, Mamta; Yadav, Swatantra Kumar; Mishra, Hirdyesh (2016). *A density functional theory insight into the structure and reactivity of diphenyltin(IV) derivative of glycylphenylalanine. Main Group Metal Chemistry, 39(3-4), –.* doi:10.1515/mgmc-2016-0009
26. Matczak, Piotr (2016). *A Test of Various Partial Atomic Charge Models for Computations on Diheteroaryl Ketones and Thioketones. Computation, 4(1), 3–.* doi:10.3390/computation4010003
27. Célia Fonseca Guerra; Jan-Willem Handgraaf; Evert Jan Baerends; F. Matthias Bickelhaupt (2004). *Voronoi deformation density (VDD) charges: Assessment of the Mulliken, Bader, Hirshfeld, Weinhold, and VDD methods for charge analysis. , 25(2), 189–210.* doi:10.1002/jcc.10351
28. Amaku Friday James*, Otuokere Ifeanyi Edozie, Theoretical Approach on Structural Aspects of a Potent, Selective, Orally Bioavailable Hedgehog Antagonist, 2-chloro-N-[4-chloro-3-(pyridin-2-yl)phenyl]-4-(methylsulfonyl)benzamide, Indian Journal of Advances in Chemical Science 4(1) (2016) 31-35
29. Thakur, V., Kumar, N., Rao, B. K., Verma, M. L., Sahu, H. D., Verma, S., & Choubey, A. K. (2021). *Density functional study on hybrid graphene/h-BN 2D sheets. Physica E: Low-Dimensional Systems and Nanostructures, 133, 114812.* doi:10.1016/j.physe.2021.11481
30. S Verma, A Kumar, H Kumar, R Baghel, N Goel, ML Verma, Ab-initio modelling for gas sensor device: based on Y-doped SnS2 monolayer Physica E: Low-dimensional Systems and Nanostructures 135, 114962, 2022, doi: 10.1016/j.physe.2021.114962
31. Perdew, John P.; Parr, Robert G.; Levy, Mel; Balduz, Jose L. (1982). *Density-Functional Theory for Fractional Particle Number: Derivative Discontinuities of the Energy. Physical Review Letters, 49(23), 1691–1694.* doi:10.1103/PhysRevLett.49.1691
32. Chattaraj, Pratim Kumar; Chakraborty, Arindam; Giri, Santanab (2009). *Net Electrophilicity. The Journal of Physical Chemistry A, 113(37), 10068–10074.* doi:10.1021/jp904674x
33. Gázquez, José L.; Cedillo, Andrés; Vela, Alberto (2007). *Electrodonating and Electroaccepting Powers. The Journal of Physical Chemistry A, 111(10), 1966–1970.* doi:10.1021/jp065459f
34. Singh, Anshika N.; Baruah, Meghna M.; Sharma, Neeti (2017). *Structure Based docking studies towards exploring potential anti-androgen activity of selected phytochemicals against Prostate Cancer. Scientific Reports, 7(1), 1955–.* doi:10.1038/s41598-017-02023-5
35. Thakur, Vishal; Kumar, Narender; Verma, Mohan L.; Choubey, Anil Kumar; Verma, Swati; Chettri, Bhanu; Sahu, Homendra D.; Rao, B. Keshav (2020). *Density functional study on hybrid h-BN/graphene atomic chains. Physica E: Low-dimensional Systems and Nanostructures, 124(), 114316–*. doi:10.1016/j.physe.2020.114316

36. Moth-Poulsen, Kasper; Bjørnholm, Thomas (2009). *Molecular electronics with single molecules in solid-state devices. , 4(9), 551–556.* doi:10.1038/nnano.2009.176
37. S. M. Lindsay; M. A. Ratner (2007). *Molecular Transport Junctions: Clearing Mists. , 19(1), 23 31.* doi:10.1002/adma.200601140

Supplementary Files

This is a list of supplementary files associated with this preprint. Click to download.

- GraphicalAbstract.docx